

1 Title: Dissecting unique and common variance across body and brain health indicators using
2 age prediction

3

4 Authors: Dani Beck^{1,2,3}, Ann-Marie G. de Lange^{3,4,5}, Tiril P. Gurholt¹, Irene Voldsbekk^{1,3},
5 Ivan I. Maximov^{1,7}, Sivaniya Subramaniapillai^{3,4}, Louise Schindler^{3,4}, Guy Hindley¹, Esten
6 H. Leonardsen^{1,3}, Zillur Rahman¹, Dennis van der Meer^{1,6}, Max Korbmacher^{1,7}, Jennifer
7 Linge^{8,9}, Olof D. Leinhard^{8,9}, Karl T. Kalleberg¹⁰, Andreas Engvig¹¹, Ida Sønnerby^{1,12,13}, Ole
8 A. Andreassen^{1,13}, Lars T. Westlye^{1,3,13}

9

10

11 ¹ NORMENT, Division of Mental Health and Addiction, Oslo University Hospital & Institute of
12 Clinical Medicine, University of Oslo, Norway

13 ² Department of Mental Health and Substance Abuse, Diakonhjemmet Hospital, Oslo, Norway

14 ³ Department of Psychology, University of Oslo, Norway

15 ⁴ LREN, Centre for Research in Neurosciences, Department of Clinical Neurosciences, CHUV and
16 University of Lausanne, Lausanne, Switzerland

17 ⁵ Department of Psychiatry, University of Oxford, Oxford, United Kingdom

18 ⁶ School of Mental Health and Neuroscience, Faculty of Health, Medicine and Life Sciences,
19 Maastricht University, Maastricht, The Netherlands

20 ⁷ Department of Health and Functioning, Western Norway University of Applied Sciences, Bergen,
21 Norway

22 ⁸ AMRA Medical AB, Linköping, Sweden

23 ⁹ Division of Diagnostics and Specialist Medicine, Department of Health, Medicine and Caring
24 Sciences, Linköping University, Linköping, Sweden

25 ¹⁰ Age Labs AS, Oslo, Norway

26 ¹¹ Department of Endocrinology, Obesity and Preventive Medicine, Section of Preventive Cardiology, Oslo
27 University Hospital, Oslo, Norway

28 ¹² Department of Medical Genetics, Oslo University Hospital, Oslo, Norway

29 ¹³ KG Jebsen Centre for Neurodevelopmental Disorders, University of Oslo

30

31

32 * Corresponding author: Dani Beck (dani.beck@psykologi.uio.no)

33

34

35

36 **Abstract**

37 Ageing is a heterogeneous multisystem process involving different rates of decline in
38 physiological integrity across biological systems. The current study dissects the unique and
39 common variance across body and brain health indicators and parses inter-individual
40 heterogeneity in the multisystem ageing process. Using machine-learning regression models
41 on the UK Biobank dataset (N = 32,593, age range 44.6-82.3, mean age 64.1 years), we first
42 estimated tissue-specific brain age for white and gray matter based on diffusion and T1-
43 weighted magnetic resonance imaging (MRI) data, respectively. Next, bodily health traits
44 including cardiometabolic, anthropometric, and body composition measures of adipose and
45 muscle tissue from bioimpedance and body MRI were combined to predict 'body age'. The
46 results showed that the body age model demonstrated comparable age prediction accuracy to
47 models trained solely on brain MRI data. The correlation between body age and brain age
48 predictions was 0.62 for the T1 and 0.64 for the diffusion-based model, indicating a degree of
49 unique variance in brain and bodily ageing processes. Bayesian multilevel modelling carried
50 out to quantify the associations between health traits and predicted age discrepancies showed
51 that higher systolic blood pressure and higher muscle-fat infiltration were related to older-
52 appearing body age compared to brain age. Conversely, higher hand-grip strength and muscle
53 volume were related to a younger-appearing body age. Our findings corroborate the common
54 notion of a close connection between somatic and brain health. However, they also suggest
55 that health traits may differentially influence age predictions beyond what is captured by the
56 brain imaging data, potentially contributing to heterogeneous ageing rates across biological
57 systems and individuals.

58

59

60

61 *Key words: Ageing, cardiometabolic, brain age, health, body composition*

62

63

64

65

66

67

68

69

70 **1. Introduction**

71 Ageing has been defined as a multisystem and time-dependent process involving progressive
72 loss of functional and physiological integrity (López-Otín et al., 2013). While advanced age
73 is a primary risk factor for cardiovascular and neurodegenerative diseases, ageing is highly
74 heterogeneous, with differential ageing rates across biological systems and individuals
75 (Cevenini et al., 2008). This has motivated a wealth of research into better understanding the
76 determinants of individual differences in ageing and its relevance to diverse disease
77 processes.

78 Several biomarkers of ageing including body composition and health traits have been
79 proposed (Cole et al., 2019). Changes in blood lipids, adipose and muscle tissue distribution,
80 blood pressure, heart rate, hand grip strength, and anthropometric measures such as body
81 mass index (BMI) and waist-to-hip ratio (WHR) are all associated with ageing (Massy-
82 Westropp et al., 2011; Mielke et al., 2010; Rodgers et al., 2019; Sebastiani et al., 2017).
83 Despite these measures being classified as markers of normal body function rather than
84 disease-specific biomarkers, recent studies have highlighted their utility for risk detection and
85 disease monitoring across cardiovascular disease and dementia (Brain et al., 2023). For
86 example, research has suggested that dysregulation in lipid metabolism in Alzheimer's
87 disease may predict cognitive decline (Wong et al., 2017).

88 Age prediction using machine learning applied to brain magnetic resonance imaging
89 (MRI) data has enabled individual-level age prediction with high accuracy based on brain
90 white (WM) and gray matter (GM) characteristics derived from diffusion and T1-weighted
91 MRI scans (Beck et al., 2021; Cole et al., 2017; Leonardsen et al., 2022), providing
92 neuroanatomical markers of brain health and integrity (Cole & Franke, 2017; Franke et al.,
93 2010). Although bodily health traits have demonstrated their influence on brain ageing (Beck,
94 de Lange, Alnæs, et al., 2022; Beck, de Lange, Pedersen, et al., 2022; de Lange et al., 2020;
95 Franke et al., 2013, 2014; Kolenic et al., 2018; Ronan et al., 2016), rates of brain and body
96 ageing processes may be partly distinct at the individual level.

97 Recent work has demonstrated the relevance of age prediction based on various organ
98 structures (Tian et al., 2023), reporting that body- and brain-specific age estimates can be
99 differentially influenced by lifestyle and environmental factors. However, a comprehensive
100 understanding of the unique and common variance across body and brain age models, in
101 addition to the contribution of specific bodily health traits, warrants further investigation. For
102 example, bodily health traits such as elevated blood pressure may potentially contribute to a

103 group-level increase in predicted age estimates relative to predictions based solely on brain
104 MRI data. However, due to the impact of elevated blood pressure on the brain (Dintica et al.,
105 2023; George et al., 2023), this variance may already to some extent be captured by brain age
106 models. The present study focuses on parsing inter-individual heterogeneity in the
107 multisystem ageing process by comparing age predictions based on models trained separately
108 on indicators of body and brain health. Specifically, we focus on identifying key health traits
109 that influence age predictions beyond the variance captured by the brain measures.

110 Using the UK Biobank sample (N = 32,593, mean age = 64.1, SD = 7.5), we assessed
111 the contributions of specific health traits to discrepancies between body and brain age
112 predictions. Bodily health traits included cardiometabolic factors, anthropometric measures,
113 and body composition measures of adipose and muscle tissue from bioimpedance and body
114 MRI. Based on documented connections between brain and body health, we anticipated that
115 age predictions based on bodily health traits would to a large extent resemble predictions
116 from models trained solely on brain MRI data. However, we expected to observe individual
117 variation in the difference between body and brain age, and that this variation would hold
118 relevant information for better understanding the role of specific health traits. Lastly, we
119 assessed the extent to which specific markers of bodily health, such as blood pressure,
120 abdominal adiposity, and muscle volume, contributed to differences in individual age
121 predictions.

122

123 **2. Methodology**

124 *2.1. Participants and ethical approval*

125 The sample was drawn from the UK Biobank (UKB) (<http://www.ukbiobank.ac.uk>). All
126 participants provided signed informed consent. UKB has IRB approval from Northwest
127 Multi-centre Research Ethics Committee and its Ethics Advisory Committee
128 (<https://www.ukbiobank.ac.uk/ethics>) oversees the UKB Ethics & Governance Framework
129 (Miller et al., 2016). Specific details regarding recruitment and data collection procedures
130 have been previously published (Collins, 2007). The present study uses the UKB Resource
131 under Application Number 27412. Participants were excluded from the present study if they
132 reported disorders that affect the brain based on ICD10 diagnoses or a long-standing illness
133 disability, diabetes, or stroke history (N = 210).

134 To remove poor-quality T1-weighted brain MRI data, participants with Euler numbers
135 (Rosen et al., 2018) ≥ 4 standard deviations below the mean were excluded. For diffusion-

136 weighted (dMRI) data, quality control was assured using the YTTTRIUM algorithm
137 (Maximov et al., 2021). A total of N = 160 participants were removed for T1 and dMRI data.
138 Body MRI measurements were quality checked by two independent, trained operators
139 visually inspecting the images prior to upload to UKB and this has been followed by control
140 of all outliers for anatomical correctness.

141 For health traits (hereby used as an umbrella term including all body composition and
142 health markers, outliers (values ± 5 SD from the mean) were excluded (N = 627) from the
143 analysis by converting the values to NA, thereby keeping the participant in the sample with
144 their respective non-outlier data. SI Figures 1 and 2 show distributions of health traits before
145 and after quality control. SI Figure 3 shows the prevalence of NA/missing data in the final
146 sample. Following cleaning, the final sample consisted of 32,593 individuals (Females: N =
147 17,200, mean age = 63.6, SD = 7.37, Males: N = 15,393, mean age = 64.71, SD = 7.63) with
148 T1, dMRI, and body health trait data. Table 1 summarises the health trait descriptive
149 statistics.

150

151 2.2. MRI data acquisition and processing

152 A detailed overview of the full UKB data acquisition and image processing protocol is
153 available in Alfaro et al. (2018) and Miller et al. (2016). Briefly, brain MRI data were
154 acquired on a 3 Tesla Siemens 32-channel Skyra scanner. T1-weighted MPRAGE volumes
155 were both acquired in sagittal orientation at $1 \times 1 \times 1$ mm³. Processing protocols followed a
156 harmonised analysis pipeline, including automated surface-based morphometry and
157 subcortical segmentation using FreeSurfer version 5.3 (Fischl et al., 2002). A standard set of
158 subcortical and cortical summary statistics were used from FreeSurfer (Fischl et al., 2002), as
159 well as a fine-grained cortical parcellation scheme (Glasser et al., 2016) to extract GM
160 cortical thickness, cortical surface area, and volume for 180 regions of interest per
161 hemisphere. This yielded a total set of 1,118 brain imaging features (360/360/360/38 for
162 cortical thickness/area/volume, as well as cerebellar/subcortical and cortical summary
163 statistics, respectively) that were used as input features in the GM-specific age prediction
164 model in line with recent implementations (de Lange et al., 2019; Kaufmann et al., 2019;
165 Schindler et al., 2022).

166 For dMRI, a conventional Stejskal-Tanner monopolar spin-echo echo-planar imaging
167 sequence was used with multiband factor 3. Diffusion weightings were 1,000 and 2,000
168 s/mm² and 50 non-coplanar diffusion directions per each diffusion shell. The spatial
169 resolution was $2 \times 2 \times 2$ mm³ isotropic, and five anterior-posterior versus three anterior-posterior

170 images with $b = 0 \text{ s/mm}^2$ were acquired. Data were processed using a previously described
 171 pipeline (Maximov et al., 2019). Metrics derived from diffusion tensor imaging (DTI)
 172 (Basser, 1995), diffusion kurtosis imaging (DKI) (Jensen et al., 2005), WM tract integrity
 173 (WMTI) (Fieremans et al., 2011), and spherical mean technique (SMT) (Kaden et al., 2016)
 174 were used as input features in the WM-specific age prediction model, as described in
 175 Voldsbekk et al. (2021). Tract-based spatial statistics (TBSS) was used to extract diffusion
 176 metrics in WM (Smith et al., 2006) (see Voldsbekk et al. (2021) for full pipeline). For each
 177 metric, WM features were extracted based on John Hopkins University (JHU) atlases for
 178 WM tracts and labels (with 0 thresholding) (Mori et al., 2006), yielding a total of 910 WM
 179 features, including mean values and regional measures for each of the diffusion model
 180 metrics, which were used as input features in the WM-specific age prediction model (Beck et
 181 al., 2021; Subramaniapillai et al., 2022; Voldsbekk et al., 2021). The diffusion MRI data
 182 passed TBSS post-processing quality control using the YTTTRIUM algorithm (Maximov et
 183 al., 2020), and were residualised with respect to scanning site using linear models.

184 The methods used to generate the body MRI-derived measurements have been
 185 described and evaluated in more detail elsewhere (Borga et al., 2018, 2020; Karlsson et al.,
 186 2015; Linge et al., 2018; West et al., 2018). Briefly, the process for fat and muscle
 187 compartments includes the following steps: (1) calibration of fat images using fat-referenced
 188 MRI, (2) registration of atlases with ground truth labels for fat and muscle compartments to
 189 the acquired MRI dataset to produce automatic segmentation, (3) quality control by two
 190 independent trained operators including the possibility to adjust and approve the final
 191 segmentation, and (4) quantification of fat volumes, muscle volumes and muscle-fat
 192 infiltration within the segmented regions. For liver proton density fat fraction (PDFF), nine
 193 regions of interest (ROI) were manually placed, evenly distributed in the liver volume, while
 194 avoiding major vessels and bile ducts. The total set of features included in the body age
 195 prediction model included 40 variables.

196

197 2.3. *Body composition and health traits*

198 Table 1 summarises the descriptive statistics of the health traits used in the study. A detailed
 199 description of each variable can be found in Supplementary Information (SI) Section 1.

200

Table 1. Descriptive statistics pertaining to each health trait, including mean \pm standard deviation (SD).

Health trait	Abbreviation	Full sample (N = 32,593)	Female (N = 17,200)	Male (N = 15,393)
--------------	--------------	-----------------------------	------------------------	----------------------

**Adipose and muscle tissue
from body MRI**

Visceral adipose tissue, <i>L</i>	VAT	3.62 ± 2.20	2.58 ± 1.48	4.78 ± 2.27
Abdominal subcutaneous adipose tissue, <i>L</i>	ASAT	6.81 ± 3.10	7.79 ± 3.30	5.72 ± 2.42
Anterior thigh muscle volume, <i>L</i>	ATMV	1.70 ± 0.48	1.34 ± 0.23	2.11 ± 0.35
Posterior thigh muscle volume, <i>L</i>	PTMV	3.36 ± 0.80	2.75 ± 0.38	4.10 ± 0.55
Anterior thigh muscle-fat infiltration, %	ATMFI	7.24 ± 1.78	7.73 ± 1.77	6.68 ± 1.62
Posterior thigh muscle-fat infiltration, %	PTMFI	10.85 ± 2.33	11.43 ± 2.26	10.18 ± 2.22
Muscle-fat infiltration, %	MFI	7.24 ± 1.78	7.73 ± 1.78	6.68 ± 1.62
Weight-to-muscle ratio, <i>kg/L</i>	WMR	7.59 ± 1.32	8.34 ± 1.21	6.73 ± 0.82
Abdominal fat ratio, %	AFR	0.49 ± 0.11	0.54 ± 0.11	0.44 ± 0.10
Liver proton density fat fraction, %	LPDF	4.03 ± 3.69	3.61 ± 3.49	4.50 ± 4.84
Total thigh muscle volume, <i>L</i>	TTMV	10.11 ± 2.52	8.19 ± 1.16	12.32 ± 1.73
Total adipose tissue volume, <i>L</i>	TAT	10.43 ± 4.45	10.37 ± 4.55	10.50 ± 4.32
Total abdominal adipose tissue index, <i>L/m²</i>	TAATi	3.64 ± 1.59	3.90 ± 1.71	3.36 ± 1.38
VAT index, <i>L/m²</i>	VATi	1.24 ± 0.71	0.98 ± 0.56	1.54 ± 0.73
ASAT index, <i>L/m²</i>	ASATi	2.42 ± 1.19	2.95 ± 1.25	1.84 ± 0.77
ATMV index, <i>L/m²</i>	ATMVi	0.59 ± 0.12	0.51 ± 0.07	0.68 ± 0.10
PTMV index, <i>L/m²</i>	PTMVi	1.63 ± 0.19	1.04 ± 0.12	1.31 ± 0.15
TTMV index, <i>L/m²</i>	TTMVi	3.50 ± 0.60	3.09 ± 0.36	3.97 ± 0.46
TAT index, <i>L/m²</i>	TATi	3.67 ± 1.60	3.93 ± 1.73	3.39 ± 1.39

**Body composition by
bioimpedance**

Body fat, %	BFP	30.85 ± 8.13	35.91 ± 6.63	25.21 ± 5.51
Whole body fat mass, <i>kg</i>	BFM	23.50 ± 8.50	25.33 ± 8.95	21.47 ± 7.44
Whole body fat free mass, <i>kg</i>	BFFM	52.08 ± 11.03	43.35 ± 4.68	61.79 ± 7.32
Body-mass index body composition, <i>kg/m²</i>	BMI-BC	26.34 ± 4.23	25.93 ± 4.57	26.80 ± 3.76
Impedance whole body, Ω	IWB	609.40 ± 88.94	665.90 ± 72.2	546.60 ± 58.57
Trunk fat, %	TFP	30.48 ± 7.59	33.20 ± 7.54	27.45 ± 6.40

**Cardiometabolic and
anthropometric**

Waist circumference, <i>cm</i>	WC	87.77 ± 12.41	82.41 ± 11.61	93.73 ± 10.38
Hip circumference, <i>cm</i>	HC	100.60 ± 8.46	100.70 ± 9.52	100.60 ± 7.09
BMI, <i>kg/m²</i>	BMI	26.32 ± 4.23	25.90 ± 4.57	26.78 ± 3.76
Hand grip strength, <i>kg</i>	HG	30.08 ± 10.18	23.04 ± 5.69	37.92 ± 8.14
Pulse, <i>bpm</i>	Pulse	68.52 ± 11.93	70.26 ± 11.35	66.59 ± 12.25
Systolic blood pressure, <i>mmHg</i>	SBP	140.5 ± 19.66	137.80 ± 20.49	143.40 ± 18.27

Diastolic blood pressure, <i>mmHg</i>	DBP	78.67 ± 10.64	76.96 ± 10.57	80.56 ± 10.39
Forced vital capacity, <i>L</i>	FVC	3.63 ± 0.93	3.05 ± 0.58	4.30 ± 0.80

Note: Bodily health traits extracted from the UKB, including adipose and muscle tissue from body MRI, body composition by bioimpedance, and cardiometabolic and anthropometric traits from physical examinations. Units are in litres (*L*), kilograms (*kg*), percent (%), centimetres (*cm*), height in metres (*m*), ohms (Ω), beats per minute (*bpm*), and millimetres of mercury (*mmHg*). For body age prediction, the model was trained with all the listed measures.

201

202 2.4. Age prediction models

203 Age prediction was carried out using XGBoost regression (eXtreme Gradient Boosting;
204 <https://github.com/dmlc/xgboost>) in Python 3.8.0, which is based on a decision-tree ensemble
205 algorithm (Chen & Guestrin, 2016) used in several recent age prediction studies (Beck, de
206 Lange, Alnæs, et al., 2022; Beck, de Lange, Pedersen, et al., 2022; Beck et al., 2021; de
207 Lange et al., 2020; Kaufmann et al., 2019; Subramaniapillai et al., 2022; Voldsbekk et al.,
208 2021). XGboost uses advanced regularisation to reduce overfitting, has shown superior
209 performance in machine learning competitions (Chen & Guestrin, 2016), and accommodates
210 the combination of health traits and brain imaging features based on FreeSurfer and FSL-
211 derived values.

212 Age prediction models were first run using only brain MRI data for WM and GM
213 features separately. Next, we ran a prediction model combining all health traits (Table 1).
214 This resulted in three age prediction models used in the current study: T1 brain age, dMRI
215 brain age, and body age. Parameters were tuned in nested cross-validations with five inner
216 folds for randomised search and 10 outer folds for validating model performance using
217 Scikit-learn (Pedregosa et al., 2011). R^2 , root mean squared error (RMSE), mean absolute
218 error (MAE), and Pearson's correlations between predicted and true values were calculated to
219 evaluate prediction accuracy. For each model, 10-fold cross-validation was used to obtain
220 brain age and body age for each individual in the full sample. SI Figure 4 shows the feature
221 importance (weight) of the variables in each age prediction model, indicating the relative
222 contribution of the corresponding feature to the prediction model. SI Table 1 shows each of
223 the variables included in the prediction models.

224

225 2.5. Difference in age predictions by bodily health traits

226 To investigate the degree to which each of the health traits influenced differences in body and
227 brain age predictions, Bayesian multilevel models were carried out in *Stan* (Stan
228 Development Team, 2023) using the *brms* (Bürkner, 2017, 2018) R-package, where

229 multivariate models are fitted in familiar syntax to comparable frequentist approaches such as
230 a linear mixed effects model using the *lme4* (Bates et al., 2015). We assessed the
231 relationships between age prediction difference scores (predicted brain age minus predicted
232 body age) and each health trait (bar body MRI index scores to reduce redundancy). For each
233 individual, a positive difference score reflects a brain age that is higher than body age, while
234 a negative difference score reflects a body age that is higher than brain age. The difference
235 score (for T1 and dMRI separately) was entered as the dependent variable, with each health
236 trait separately entered as the independent fixed effects variable along with age and sex, with
237 subject ID as the random effect:

238

239 $Age\ prediction\ difference\ score \sim Health\ trait + Age + Sex (1|SubjectID)$ (1)

240

241 To prevent false positives and to regularise the estimated associations, we defined a
242 standard prior around zero with a standard deviation of 0.3 for all coefficients, reflecting a
243 baseline expectation of effects being small but allowing for sufficient flexibility in
244 estimation. All variables bar sex were standardised before running the analyses. Each model
245 was run with 8000 iterations, including 4000 warmup iterations, across four chains. This
246 setup was chosen to ensure robust convergence and adequate sampling from the posterior
247 distributions. For each coefficient of interest, we report the mean estimated value of the
248 posterior distribution (β) and its 95% credible interval (the range of values that with 95%
249 confidence contains the true value of the association), and calculated the Bayes Factor (BF) –
250 provided as evidence ratios in the presented figures – using the Savage-Dickey method
251 (Wagenmakers et al., 2010). Briefly, BF can be interpreted as a measure of the strength of
252 evidence (*extreme, very strong, strong, moderate, anecdotal, none*) in favour of the null or
253 alternative hypothesis. For a pragmatic guide on BF interpretation, see SI Table 2.

254

255 **3. Results**

256 *3.1. Brain age and body age prediction*

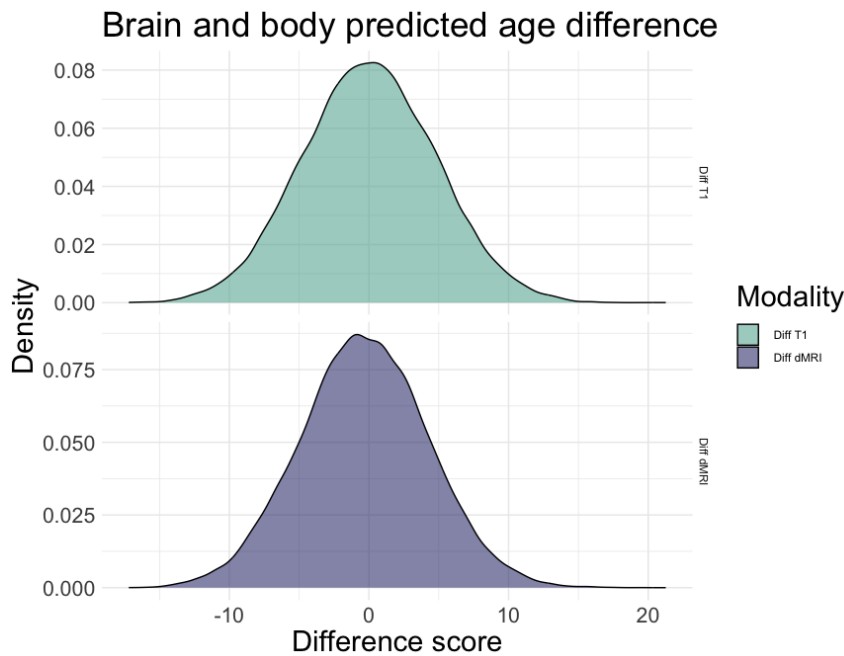
257 Table 2 summarises descriptive and model validation statistics pertaining to each age
258 prediction model. Figure 1 shows the distributions of the age prediction difference scores
259 (predicted T1/dMRI brain age minus predicted body age). SI Figure 5 shows the correlation
260 between the T1 and dMRI-based brain age versus body age difference scores. Figure 2 shows
261 a correlation matrix including the three models' predicted ages and age gaps. See SI Figure 6

262 for correlation matrix showing the association between health traits and SI Figure 7 for
 263 predicted age as a function of chronological age for each age prediction model.
 264
 265

Table 2. Average R^2 , root mean square error (RMSE), mean absolute error (MAE) standard deviation, and Pearson's correlations between predicted and true age (r) for each age prediction model. 95% confidence intervals on r are calculated using Fisher's z-transformation, adjusted for sample size, and back-transformed to the original scale.

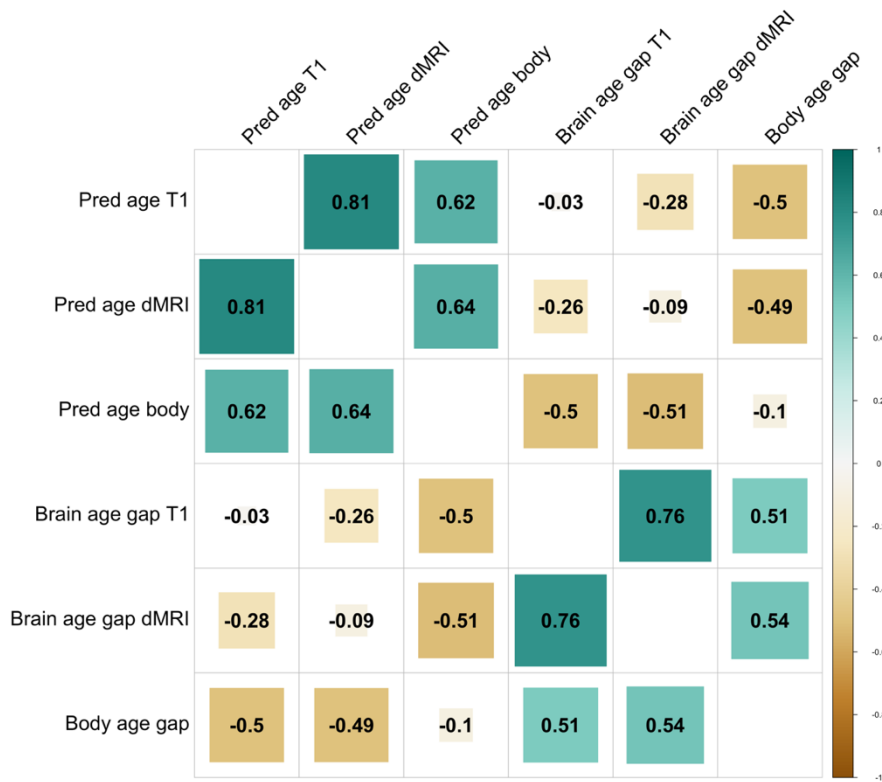
	T1 brain age	dMRI brain age	Body age
r	0.76 [0.755, 0.764]	0.77 [0.765, 0.773]	0.78 [0.778, 0.786]
r^2	0.57 ± 0.015	0.62 ± 0.007	0.59 ± 0.044
RMSE	4.93 ± 0.058	4.67 ± 0.120	4.70 ± 0.151
MAE	3.94 ± 0.054	3.70 ± 0.070	3.73 ± 0.113

266



267

268 **Figure 1.** Age difference score distribution (density) for T1 (Diff T1) and dMRI (Diff dMRI) weighted age
 269 models. Mean difference scores = 0.028 (T1) and -4.33 (dMRI), with standard deviation (SD) of 4.78 and 4.58,
 270 respectively.



272

273 **Figure 2.** Correlation matrix showing the associations between the predicted ages and age gaps of the three
 274 models.

275

276 *3.2. Bayesian multilevel models*

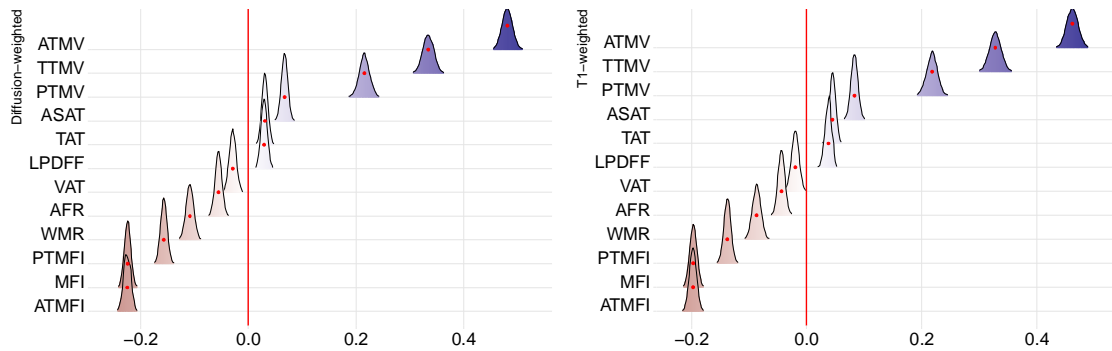
277 Bayesian multilevel modelling tested the associations between each bodily health trait and
 278 the difference score (brain-predicted age minus body-predicted age). Due to the large number
 279 of included health traits, we present associations between 1) age prediction difference and
 280 body MRI measures and 2) age prediction difference and cardiometabolic, anthropometric
 281 and bioimpedance measures separately below. The full results are available in SI Tables 3
 282 and 4. For estimated credible intervals, see SI Figures 8 and 9. See SI Table 5 for full and
 283 partial linear regressions between age and each of the health trait adjusted for brain-predicted
 284 age. See SI Figures 10 and 11 for scatterplots and Pearson’s R reflecting each of the
 285 associations between health traits and difference scores between brain age and body age
 286 models and SI Figure 12 for scatterplots reflecting associations between health traits and
 287 body age gap. Sensitivity analyses using linear mixed effects models showing the results with
 288 age-bias corrected scores versus uncorrected scores but with age as a covariate are provided
 289 in SI Figures 13 and 14.

290

291 *3.2.1. Difference scores and body MRI features*

292 Figure 3 shows posterior distributions reflecting the associations between each body MRI
293 feature and the age prediction difference scores. Values increasing from 0 to 1 show evidence
294 of a positive association (where higher values on health traits relate to lower body age
295 relative to brain age) and values decreasing 0 to -1 show evidence of a negative association
296 (where higher values on health traits relate to higher body age relative to brain age).

297



298

299 **Figure 3. Associations between body MRI features and difference scores between brain-age models and**
300 **body-age models (dMRI and T1).** The figure shows posterior distributions of the estimates of the standardised
301 coefficient. Estimates for each body MRI feature on dMRI difference score on the left and T1-weighted
302 difference score on the right. Colour scale follows the directionality of evidence, with positive (blue) values
303 indicating evidence in favour of positive associations (i.e., larger brain than body age) and negative (red) values
304 indicating evidence in favour of negative associations (i.e., larger body than brain age). The width of the
305 distribution represents the uncertainty of the parameter estimates. For a list of unabbreviated words, see Table 1.

306

307 For both dMRI and T1 age difference scores, the tests revealed evidence of a positive
308 association with predicted age difference score (calculated as brain age – body age) for
309 ATMV (dMRI: BF < 0.001, $\beta = 0.48$; T1: BF < 0.001, $\beta = 0.46$), TTMV (dMRI: BF < 0.001,
310 $\beta = 0.33$; T1: BF < 0.001, $\beta = 0.33$), PTMV (dMRI: BF < 0.001, $\beta = 0.22$; T1: BF < 0.001, β
311 = 0.22), ASAT (dMRI: BF < 0.001, $\beta = 0.07$; T1: BF < 0.001, $\beta = 0.08$), TAT (dMRI: BF <
312 0.001, $\beta = 0.03$; T1: BF < 0.001, $\beta = 0.05$), and LPDF (dMRI: BF < 0.001, $\beta = 0.03$; T1:
313 BF < 0.001, $\beta = 0.04$), indicating that higher levels of muscle volume in the thighs, especially
314 anterior, is associated with a positive difference score (i.e., higher predicted brain age than
315 body age; high muscle volume relations with younger-appearing body ageing).

316

317 The tests also revealed evidence of a negative association with predicted age
318 difference score for ATMFI (dMRI: BF < 0.001, $\beta = -0.23$; T1: BF < 0.001, $\beta = -0.20$),
PTMFI (dMRI: BF < 0.001, $\beta = -0.16$; T1: BF < 0.001, $\beta = -0.14$), MFI (dMRI: BF < 0.001,

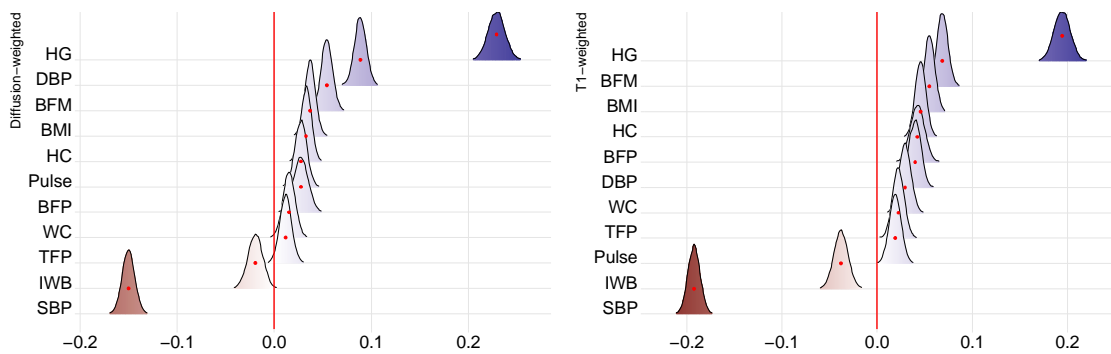
319 $\beta = -0.23$; T1: BF < 0.001, $\beta = -0.20$), WMR (dMRI: BF < 0.001, $\beta = -0.11$; T1: BF < 0.001,
 320 $\beta = -0.08$), and AFR (dMRI: BF < 0.001, $\beta = -0.06$; T1: BF < 0.001, $\beta = -0.04$), indicating
 321 that higher fat infiltration in the muscles, especially the anterior thighs, were associated with
 322 a negative difference score (i.e., higher predicted body age than brain age). There was also
 323 evidence of a negative association for dMRI VAT (BF < 0.001, $\beta = -0.03$) and no association
 324 for T1 VAT (BF = 0.30, $\beta = -0.02$).

325

326 3.2.2. Difference scores and cardiometabolic, anthropometric and bioimpedance

327 Figure 4 shows posterior distributions reflecting the associations between cardiometabolic,
 328 anthropometric, and bioimpedance traits and the age prediction difference scores.

329



330

331 **Figure 4. Associations between cardiometabolic, anthropometric, and bioimpedance traits and difference**
 332 **score between brain age models (dMRI and T1) and body age model.** The figure shows posterior
 333 distributions of the estimates of the standardised coefficient. Estimates for each health trait on dMRI difference
 334 score on the left and T1-weighted difference score on the right.

335

336 For both dMRI and T1 age difference scores, the tests revealed evidence of a positive
 337 association with age prediction difference scores for HC (dMRI: BF < 0.001, $\beta = 0.03$; T1:
 338 BF < 0.001, $\beta = 0.05$), DBP (dMRI: BF < 0.001, $\beta = 0.09$; T1: BF < 0.001, $\beta = 0.04$), BFP
 339 (dMRI: BF = 0.05, $\beta = 0.03$; T1: BF < 0.001, $\beta = 0.04$), HG (dMRI: BF < 0.001, $\beta = 0.23$;
 340 T1: BF < 0.001, $\beta = 0.19$), BFM (dMRI: BF < 0.001, $\beta = 0.05$; T1: BF < 0.001, $\beta = 0.07$),
 341 and BMI (dMRI: BF < 0.001, $\beta = 0.04$; T1: BF < 0.001, $\beta = 0.06$). There was also a positive
 342 association for dMRI Pulse (BF = 0.006, $\beta = 0.03$), T1 WC (BF < 0.001, $\beta = 0.03$), and T1
 343 TFP (BF = 0.015, $\beta = 0.02$), but not for corresponding T1 Pulse (BF = 0.455, $\beta = 0.02$),
 344 dMRI WC (BF < 2.798, $\beta = 0.02$), and dMRI TFP (BF < 7.783, $\beta = 0.01$).

345

346 In terms of negative associations with age prediction difference scores, effects were
 found for SBP for both modalities (dMRI: BF < 0.001, $\beta = -0.15$; T1: BF < 0.001, $\beta = -0.19$),

347 and T1 IWB ($BF < 0.001$, $\beta = -0.04$), but not dMRI IWB ($BF = 1.226$, $\beta = -0.02$). The results
348 indicate that high levels of various measures of adiposity and hand grip strength are
349 associated with a higher brain age than body age, with beta coefficients showing the strongest
350 effect for hand grip strength. Systolic blood pressure is implicated as the largest contributor
351 to higher body predicted age.

352

353 **4. Discussion**

354 Evidence of differential ageing rates across different biological systems in the same
355 individual (Cevenini et al., 2008) has led us to conceptualise ageing as a mosaic and
356 heterogeneous construct. One implication is that individual biomarkers studied in isolation
357 may not accurately reflect risk of disease or outcome (Sebastiani et al., 2017), and the use of
358 multiple models in coherence has been recommended (Cevenini et al., 2008; Cole et al.,
359 2019; Kuo et al., 2021). Our analyses revealed that an age prediction model trained on bodily
360 health traits rendered comparably high prediction accuracy compared to the models trained
361 solely on brain MRI data. However, only moderate correlations between body age and brain
362 age predictions were found, indicating a degree of unique variance in brain and bodily ageing
363 processes. Multilevel modelling showed that several elevated body health risk traits
364 differentially contributed to a group level increase or decrease in predicted age, potentially
365 revealing unique and common influences of bodily health traits on body and brain ageing
366 systems.

367 We ran Bayesian multilevel modelling to quantify the associations between the
368 predicted age difference score and each of the health traits. The results are largely in line with
369 our expectations of measures related to poorer and better somatic health having differential
370 contributions to our age models, whereby poor health is manifested as older-appearing body
371 age and better health as younger-appearing body age. In parsing unique and common
372 influences of different health traits on brain and bodily ageing, we interpret traits with
373 moderate effects on the age prediction difference scores as likely having more of a unique
374 contribution to brain or bodily ageing. For example, the results indicate that thigh muscle
375 volume and hand grip strength showed a larger effect on younger-appearing body ages
376 relative to brain ages, as compared to e.g., liver fat, subcutaneous fat, diastolic blood
377 pressure, BMI, hip and waist circumference, which showed negligible beta coefficients (see
378 Figures 3 and 4 and SI Tables 3 and 4). The latter measures may thus represent health traits
379 that are less likely to uniquely influence brain or bodily ageing while measures related to
380 muscular fitness have a larger impact on a younger body age. Conversely, muscle-fat

381 infiltration and systolic blood pressure have a larger effect on older-appearing body ages
382 relative to brain ages.

383 However, some findings remain difficult to interpret. For example, we found opposite
384 associations for systolic versus diastolic blood pressure. Previous research has also reported
385 inconsistent effects, with a UKB study reporting higher SBP and DBP associations with
386 greater and lower risk of dementia respectively (Gong et al., 2021). There are also several
387 adiposity-related health traits with positive associations (indicating older-appearing brain age
388 than body age). While these have negligible beta coefficients, the results may be
389 counterintuitive and, based on an extensive literature on the negative effects of obesity, we
390 would typically expect higher adiposity to be related to older-appearing body age relative to
391 the brain. However, other studies have reported similar findings, for example greater scores
392 on anthropometric measures associated with better health outcomes – often referred to as ‘the
393 obesity paradox’ (Amundson et al., 2010; Tutor et al., 2023). While such findings might be
394 influenced by different adiposity measures used across studies (Bosello & Vanzo, 2021) as
395 well as selection biases (Ba et al., 2012; Masters et al., 2013), future research might focus on
396 variations in body-brain relationships across age, sex, and health status (Kivimäki et al.,
397 2018; Subramaniapillai et al., 2022) to better understand these relationships.

398 An individual may have a brain-predicted age closely aligned with their chronological
399 age but a body age that exceeds it. One theoretical explanation for this may be the
400 involvement of brain maintenance (Nyberg, 2017), where brain health may to some extent be
401 preserved irrespective of bodily health status through a moderating variable such as good
402 muscular fitness. Furthermore, individual differences in cognitive reserve (Stern, 2009,
403 2012), or resilience to neuropathological changes typically associated with ageing, could
404 influence differences in age-prediction scores. Future studies might therefore aim to
405 investigate these difference scores in the context of cognitive functions known to change with
406 age, such as memory and reaction time (Grady, 2012), as well as reserve-related mechanisms
407 including education, socioeconomic status, and lifestyle (Anatürk et al., 2021). Although
408 speculative, higher body age than brain age may reflect worsening bodily health that has not
409 yet manifested in the brain, which may represent a window of opportunity for intervention.
410 This emphasises the importance of future longitudinal studies. Moreover, it is important to
411 note that a high brain and body age discrepancy does not necessarily mean an old brain and a
412 young body or vice versa, but rather that the brain age is higher or lower relative to the body
413 age. Hence, both brain and body age could be both higher or lower than individual’s
414 chronological age. Future studies may test the relevance of different brain and body age

415 configurations, with the aim to characterise distinct risk profiles related to neural and
416 cardiometabolic health.

417 Previous studies have demonstrated that variation in predicted brain age is partly
418 explained by individual differences in body composition and health traits, including
419 abdominal fat (Beck, de Lange, Pedersen, et al., 2022; Schindler et al., 2022;
420 Subramaniapillai et al., 2022), muscle-fat infiltration (Beck, de Lange, Alnæs, et al., 2022),
421 hand-grip strength (Cole et al., 2018; Sanders et al., 2021) and muscle volume (Beck, de
422 Lange, Alnæs, et al., 2022). Our findings support these previous reports, but also suggest that
423 health traits may differentially influence age predictions beyond what is captured by the brain
424 imaging measures. However, it could also be the case that the health trait variables do not
425 influence the estimated age in a specific direction on their own, but rather, that the variation
426 reflects the extent to which the given variable is already integrated into the individual's brain
427 health. Consequently, the difference score would represent a value indicative of the
428 individual in question rather than providing a generalised insight about the health trait itself.
429 There are also a wide range of related health, lifestyle, and environmental factors that our
430 study did not include such as diet, physical activity, socio-economic status, education, social
431 support, and access to healthcare, which may mitigate the effects of our results or reveal
432 larger discrepancies. Future research might consider these aspects by stratifying samples
433 based on different levels of education and lifestyle behaviours, or adjust for the effects of
434 these variables in follow-up analyses.

435 Further, the correlation (SI Figure 5) between the difference scores in T1- and dMRI-
436 based models indicate that the difference in predictions are related but not identical. As
437 evidenced by Figures 3 and 4, most of our findings related to difference scores were similar
438 across brain MRI modalities. However, for a few select variables, the results suggest there
439 may be some tissue-specific effects. For example, dMRI-Pulse, T1-WC, T1-TFP revealed
440 positive associations while there were no effects for their counterparts (T1-Pulse, dMRI-WC,
441 dMRI-TFP). Similarly, there were negative associations for dMRI-VAT and T1-IWB but no
442 effects for T1-VAT or dMRI-IWB. While these results could reflect subtle, differential
443 discrepancies between tissue-specific neural ageing processes and body age, it is important to
444 note that these discrepancies between imaging modalities may be trivial, as the reported
445 findings for these variables reflect anecdotal evidence. In addition, the large sample size
446 (~40k) and power of the study which may lead to even trivial differences and small effects
447 being detected as statistically significant. As such, we focus on the beta coefficients and
448 strength of evidence derived from those values to make more practical conclusions. Future

449 studies may consider more comprehensive investigations of tissue-specific and regional MRI
450 phenotypes that may be uniquely associated with discrepancies in brain and body age
451 predictions.

452 Some strengths and limitations of the study must be discussed. The UK Biobank
453 offers a rich and comprehensive dataset enriched with health-related information, including
454 lifestyle and health factors utilised in the current study. However, selection biases (Brayne &
455 Moffitt, 2022; Tyrrell et al., 2021) such as overall relatively higher education and
456 overrepresentation by individuals of white European descent makes the sample less
457 representative of the wider population. One argument in favour of recruiting relatively
458 healthy individuals at baseline is that some will develop illnesses over the course of the study
459 period, allowing researchers to track changes over time and identify predictors of health
460 decline and therefore targets for intervention strategies. However, our cross-sectional study
461 may be influenced by healthy-volunteer bias, limiting the representativeness of the sample in
462 terms of cardiovascular risk in midlife and older age. A further limitation of the UK Biobank
463 is the limited age range, with participants involved being between 44-82 years of age. Given
464 the importance of tracking changes over time and the potential differences in how bodily
465 health traits may relate to brain health across the lifespan (Kivimäki et al., 2018), and that this
466 may also vary between males and females (Subramaniapillai et al., 2022), future research
467 should include sex-specific models, wider age ranges, and preferably longitudinal data on
468 more diverse and representative samples.

469 In terms of age prediction, all three models performed comparably well, both in terms
470 of r values and MAE and RSME. However, while brain-based age models had approximately
471 1000 features, the body age model only included 40. This variation in features warrants
472 caution in interpreting model differences as being driven strictly by biological mechanisms.
473 That said, while prediction accuracies can improve with a larger number of features included,
474 this is not always the case. For example, in Tian et al. (2023), the least accurate organ-
475 specific model included the largest number of features ($n = 33$) and the best performing
476 model including 11 features. Similarly, our previous studies show that the age-dependency of
477 features may be more indicative of model performance than the sheer number of features
478 included (Anatürk et al., 2021; de Lange et al., 2020), highlighting the importance of feature
479 relevance over quantity in predictive accuracy. This underscores the need for further research
480 to validate age prediction models related to bodily health and organ systems, assessing the
481 optimal balance and significance of feature number versus their age-related associations.

482 Although we employed nested cross-validation and k-folding to limit overfitting and
483 generate predictions for the full sample in a held-out manner, our models may not generalise
484 due to the lack of external datasets for validation. Moreover, investigating which body-age
485 features drive the discrepancy between brain and body age predictions, whereby the same set
486 of health traits were used to train the body age model, may introduce circularity. Future
487 research may improve generalisability by including independent samples for validation, as
488 well as more comprehensive approaches to assessing brain- versus body-related age
489 predictions and model feature importance. While we provide feature importance based on
490 model weight scores for transparency, inherent limitations in assessing feature importance
491 limit the generalisability of these rankings (Haufe et al., 2014). For example, weight and gain
492 metrics may bias towards features with higher cardinality, or exclude equally age-dependent
493 features from the model due to multicollinearity (Adler & Painsky, 2022). Additionally, these
494 methods often overlook complex feature interactions and the nonlinear nature of models like
495 XGBoost, leading to potential misinterpretation (Goyal et al., 2020). To enhance model
496 transparency and interpretability, future studies might aim to address these challenges by
497 incorporating permutation feature importance, SHAP values, and partial dependence plots
498 (Altmann et al., 2010; Lundberg & Lee, 2017), alongside external validation on independent
499 datasets as well as pre-modeling strategies like principal component analysis (PCA) to
500 mitigate multicollinearity. Lastly, deep neural network models for age prediction have shown
501 superior performance in recent years (Leonardsen et al., 2022) and should be considered to
502 improve robustness of the methodology.

503 To summarise, we found that age prediction using bodily health traits performed
504 comparably well to models using brain MRI data alone, and that specific health traits may
505 differentially influence brain and body ageing systems. Our results emphasise the relevance
506 of considering both body and brain measures for a more comprehensive understanding of
507 biological ageing. The current study thus contributes to the dissection of the unique and
508 common variance across body and brain health indicators, which is key towards the aim of
509 parsing inter-individual heterogeneity in the multisystem ageing process. Future research
510 should attempt to better understand the clinical relevance of individual-level discrepancies
511 between different age prediction models in relation to early life exposures, lifestyle factors,
512 genetic architecture, and their relation to risk for cardiovascular disease and age-related
513 neurodegenerative and cognitive disorders.

514

515 **5. Data availability**

516 The UK Biobank resource is open for eligible researchers upon application
517 (<http://www.ukbiobank.ac.uk/register-apply/>).

518

519

520

521 **6. Funding and acknowledgements**

522 The Research Council of Norway (#223273, #324252, #300767, #324499); South-Eastern
523 Norway Regional Health Authority (#2017112; #2019101, #2022080, #2020060); European
524 Union's Horizon 2020 Research and Innovation Programme (CoMorMent project, Grant
525 #847776; BRAINMINT project, Grant #802998), the German Federal Ministry of Education
526 and Research (01ZX1904A), and the Swiss National Science Foundation (#PZ00P3_193658,
527 #TMPFP3_217174). We performed this work on the *Services for sensitive data* (TSD),
528 University of Oslo, Norway, with resources provided by UNINETT Sigma2 - the National
529 Infrastructure for High-Performance Computing and Data Storage in Norway. We conducted
530 this research using the UK Biobank Resource under Application Number 27412.

531

532 **7. Declaration of competing interests**

533 OAA is a consultant to cortechs.ai and received speaker's honorarium from Lundbeck,
534 Janssen and Sunovion unrelated to the topic of the current study. JL is an employee and
535 shareholder of AMRA Medical AB and reports consulting and speaking honoraria from Eli
536 Lilly and BioMarin unrelated to the topic of the current study. ODL is an employee and
537 shareholder of AMRA Medical AB and reports consulting from Eli Lilly and Fulcrum
538 Therapeutics unrelated to the topic of the current study.

539

540 **8. References**

541 Adler, A. I., & Painsky, A. (2022). Feature Importance in Gradient Boosting Trees with

542 Cross-Validation Feature Selection. *Entropy*, *24*(5), Article 5.

543 <https://doi.org/10.3390/e24050687>

544 Alfaro, F. J., Gavrieli, A., Saade-Lemus, P., Lioutas, V.-A., Upadhyay, J., & Novak, V.

545 (2018). White matter microstructure and cognitive decline in metabolic syndrome: A

546 review of diffusion tensor imaging. *Metabolism: Clinical and Experimental*, *78*, 52–

547 68. <https://doi.org/10.1016/j.metabol.2017.08.009>

548 Altmann, A., Toloşi, L., Sander, O., & Lengauer, T. (2010). Permutation importance: A
549 corrected feature importance measure. *Bioinformatics*, 26(10), 1340–1347.
550 <https://doi.org/10.1093/bioinformatics/btq134>

551 Amundson, D. E., Djurkovic, S., & Matwiyoff, G. N. (2010). The Obesity Paradox. *Critical*
552 *Care Clinics*, 26(4), 583–596. <https://doi.org/10.1016/j.ccc.2010.06.004>

553 Anatürk, M., Kaufmann, T., Cole, J. H., Suri, S., Griffanti, L., Zsoldos, E., Filippini, N.,
554 Singh-Manoux, A., Kivimäki, M., Westlye, L. T., Ebmeier, K. P., & Lange, A.-M. G.
555 de. (2021). Prediction of brain age and cognitive age: Quantifying brain and cognitive
556 maintenance in aging. *Human Brain Mapping*, 42(6), 1626–1640.
557 <https://doi.org/10.1002/hbm.25316>

558 Ba, G., Vt, C., Ma, E., S, K., Hl, W., & Mh, C. (2012). The older the better: Are elderly study
559 participants more non-representative? A cross-sectional analysis of clinical trial and
560 observational study samples. *BMJ Open*, 2(6). [https://doi.org/10.1136/bmjopen-2012-](https://doi.org/10.1136/bmjopen-2012-000833)
561 [000833](https://doi.org/10.1136/bmjopen-2012-000833)

562 Basser, P. J. (1995). Inferring microstructural features and the physiological state of tissues
563 from diffusion-weighted images. *NMR in Biomedicine*, 8(7), 333–344.
564 <https://doi.org/10.1002/nbm.1940080707>

565 Bates, D., Mächler, M., Bolker, B., & Walker, S. (2015). Fitting Linear Mixed-Effects
566 Models Using **lme4**. *Journal of Statistical Software*, 67(1).
567 <https://doi.org/10.18637/jss.v067.i01>

568 Beck, D., de Lange, A.-M. G., Alnæs, D., Maximov, I. I., Pedersen, M. L., Leinhard, O. D.,
569 Linge, J., Simon, R., Richard, G., Ulrichsen, K. M., Dørum, E. S., Kolskår, K. K.,
570 Sanders, A.-M., Winterton, A., Gurholt, T. P., Kaufmann, T., Steen, N. E., Nordvik, J.
571 E., Andreassen, O. A., & Westlye, L. T. (2022). Adipose tissue distribution from body

572 MRI is associated with cross-sectional and longitudinal brain age in adults.
573 *NeuroImage: Clinical*, 33, 102949. <https://doi.org/10.1016/j.nicl.2022.102949>

574 Beck, D., de Lange, A.-M. G., Maximov, I. I., Richard, G., Andreassen, O. A., Nordvik, J. E.,
575 & Westlye, L. T. (2021). White matter microstructure across the adult lifespan: A
576 mixed longitudinal and cross-sectional study using advanced diffusion models and
577 brain-age prediction. *NeuroImage*, 224, 117441.
578 <https://doi.org/10.1016/j.neuroimage.2020.117441>

579 Beck, D., de Lange, A.-M. G., Pedersen, M. L., Alnæs, D., Maximov, I. I., Voldsbekk, I.,
580 Richard, G., Sanders, A.-M., Ulrichsen, K. M., Dørum, E. S., Kolskår, K. K.,
581 Høgestøl, E. A., Steen, N. E., Djurovic, S., Andreassen, O. A., Nordvik, J. E.,
582 Kaufmann, T., & Westlye, L. T. (2022). Cardiometabolic risk factors associated with
583 brain age and accelerate brain ageing. *Human Brain Mapping*, 43(2), 700–720.
584 <https://doi.org/10.1002/hbm.25680>

585 Borga, M., Ahlgren, A., Romu, T., Widholm, P., Dahlqvist Leinhard, O., & West, J. (2020).
586 Reproducibility and repeatability of MRI-based body composition analysis. *Magnetic
587 Resonance in Medicine*, 84(6), 3146–3156. <https://doi.org/10.1002/mrm.28360>

588 Borga, M., West, J., Bell, J. D., Harvey, N. C., Romu, T., Heymsfield, S. B., & Dahlqvist
589 Leinhard, O. (2018). Advanced body composition assessment: From body mass index
590 to body composition profiling. *Journal of Investigative Medicine: The Official
591 Publication of the American Federation for Clinical Research*, 66(5), 1–9.
592 <https://doi.org/10.1136/jim-2018-000722>

593 Bosello, O., & Vanzo, A. (2021). Obesity paradox and aging. *Eating and Weight Disorders -
594 Studies on Anorexia, Bulimia and Obesity*, 26(1), 27–35.
595 <https://doi.org/10.1007/s40519-019-00815-4>

596 Brain, J., Greene, L., Tang, E. Y. H., Louise, J., Salter, A., Beach, S., Turnbull, D., Siervo,
597 M., Stephan, B. C. M., & Tully, P. J. (2023). Cardiovascular disease, associated risk
598 factors, and risk of dementia: An umbrella review of meta-analyses. *Frontiers in*
599 *Epidemiology*, 3. <https://www.frontiersin.org/articles/10.3389/fepid.2023.1095236>

600 Brayne, C., & Moffitt, T. E. (2022). The limitations of large-scale volunteer databases to
601 address inequalities and global challenges in health and aging. *Nature Aging*, 2(9),
602 Article 9. <https://doi.org/10.1038/s43587-022-00277-x>

603 Bürkner, P.-C. (2017). **brms**: An R Package for Bayesian Multilevel Models Using *Stan*.
604 *Journal of Statistical Software*, 80(1). <https://doi.org/10.18637/jss.v080.i01>

605 Bürkner, P.-C. (2018). Advanced Bayesian Multilevel Modeling with the R Package brms.
606 *The R Journal*, 10(1), 395. <https://doi.org/10.32614/RJ-2018-017>

607 Cevenini, E., Invidia, L., Lescai, F., Salvioli, S., Tieri, P., Castellani, G., & Franceschi, C.
608 (2008). Human models of aging and longevity. *Expert Opinion on Biological*
609 *Therapy*, 8(9), 1393–1405. <https://doi.org/10.1517/14712598.8.9.1393>

610 Chen, T., & Guestrin, C. (2016). XGBoost: A Scalable Tree Boosting System. *Proceedings*
611 *of the 22nd ACM SIGKDD International Conference on Knowledge Discovery and*
612 *Data Mining*, 785–794. <https://doi.org/10.1145/2939672.2939785>

613 Cole, & Franke, K. (2017). Predicting Age Using Neuroimaging: Innovative Brain Ageing
614 Biomarkers. *Trends in Neurosciences*, 40(12), 681–690.
615 <https://doi.org/10.1016/j.tins.2017.10.001>

616 Cole, J. H., Marioni, R. E., Harris, S. E., & Deary, I. J. (2019). Brain age and other bodily
617 ‘ages’: Implications for neuropsychiatry. *Molecular Psychiatry*, 24(2), 266–281.
618 <https://doi.org/10.1038/s41380-018-0098-1>

619 Cole, J. H., Poudel, R. P. K., Tsagkrasoulis, D., Caan, M. W. A., Steves, C., Spector, T. D., &
620 Montana, G. (2017). Predicting brain age with deep learning from raw imaging data

621 results in a reliable and heritable biomarker. *NeuroImage*, 163, 115–124.
622 <https://doi.org/10.1016/j.neuroimage.2017.07.059>

623 Cole, J. H., Ritchie, S. J., Bastin, M. E., Hernández, M. C. V., Maniega, S. M., Royle, N.,
624 Corley, J., Pattie, A., Harris, S. E., Zhang, Q., Wray, N. R., Redmond, P., Marioni, R.
625 E., Starr, J. M., Cox, S. R., Wardlaw, J. M., Sharp, D. J., & Deary, I. J. (2018). Brain
626 age predicts mortality. *Molecular Psychiatry*, 23(5), 1385–1392.
627 <https://doi.org/10.1038/mp.2017.62>

628 Collins, R. (2007). *UK Biobank Protocol*.

629 de Lange, A.-M. G., Anatórk, M., Suri, S., Kaufmann, T., Cole, J. H., Griffanti, L., Zsoldos,
630 E., Jensen, D. E. A., Filippini, N., Singh-Manoux, A., Kivimäki, M., Westlye, L. T.,
631 & Ebmeier, K. P. (2020). Multimodal brain-age prediction and cardiovascular risk:
632 The Whitehall II MRI sub-study. *NeuroImage*, 222, 117292.
633 <https://doi.org/10.1016/j.neuroimage.2020.117292>

634 de Lange, A.-M. G., Kaufmann, T., van der Meer, D., Maglanoc, L. A., Alnæs, D., Moberget,
635 T., Douaud, G., Andreassen, O. A., & Westlye, L. T. (2019). Population-based
636 neuroimaging reveals traces of childbirth in the maternal brain. *Proceedings of the*
637 *National Academy of Sciences*, 116(44), 22341–22346.
638 <https://doi.org/10.1073/pnas.1910666116>

639 Dintica, C. S., Habes, M., Erus, G., Vittinghoff, E., Davatzikos, C., Nasrallah, I. M., Launer,
640 L. J., Sidney, S., & Yaffe, K. (2023). Elevated blood pressure is associated with
641 advanced brain aging in mid-life: A 30-year follow-up of The CARDIA Study.
642 *Alzheimer's & Dementia*, 19(3), 924–932. <https://doi.org/10.1002/alz.12725>

643 Fieremans, E., Jensen, J. H., & Helpert, J. A. (2011). White matter characterization with
644 diffusional kurtosis imaging. *NeuroImage*, 58(1), 177–188.
645 <https://doi.org/10.1016/j.neuroimage.2011.06.006>

646 Fischl, B., Salat, D. H., Busa, E., Albert, M., Dieterich, M., Haselgrove, C., van der Kouwe,
647 A., Killiany, R., Kennedy, D., Klaveness, S., Montillo, A., Makris, N., Rosen, B., &
648 Dale, A. M. (2002). Whole Brain Segmentation. *Neuron*, 33(3), 341–355.
649 [https://doi.org/10.1016/S0896-6273\(02\)00569-X](https://doi.org/10.1016/S0896-6273(02)00569-X)

650 Franke, K., Gaser, C., Manor, B., & Novak, V. (2013). Advanced BrainAGE in older adults
651 with type 2 diabetes mellitus. *Frontiers in Aging Neuroscience*, 5.
652 <https://doi.org/10.3389/fnagi.2013.00090>

653 Franke, K., Ristow, M., & Gaser, C. (2014). Gender-specific impact of personal health
654 parameters on individual brain aging in cognitively unimpaired elderly subjects.
655 *Frontiers in Aging Neuroscience*, 6. <https://doi.org/10.3389/fnagi.2014.00094>

656 Franke, K., Ziegler, G., Klöppel, S., & Gaser, C. (2010). Estimating the age of healthy
657 subjects from T1-weighted MRI scans using kernel methods: Exploring the influence
658 of various parameters. *NeuroImage*, 50(3), 883–892.
659 <https://doi.org/10.1016/j.neuroimage.2010.01.005>

660 George, K. M., Maillard, P., Gilsanz, P., Fletcher, E., Peterson, R. L., Fong, J., Mayeda, E.
661 R., Mungas, D. M., Barnes, L. L., Glymour, M. M., DeCarli, C., & Whitmer, R. A.
662 (2023). Association of Early Adulthood Hypertension and Blood Pressure Change
663 With Late-Life Neuroimaging Biomarkers. *JAMA Network Open*, 6(4), e236431.
664 <https://doi.org/10.1001/jamanetworkopen.2023.6431>

665 Glasser, M. F., Coalson, T. S., Robinson, E. C., Hacker, C. D., Harwell, J., Yacoub, E.,
666 Ugurbil, K., Andersson, J., Beckmann, C. F., Jenkinson, M., Smith, S. M., & Van
667 Essen, D. C. (2016). A multi-modal parcellation of human cerebral cortex. *Nature*,
668 536(7615), Article 7615. <https://doi.org/10.1038/nature18933>

669 Gong, J., Harris, K., Peters, S. A. E., & Woodward, M. (2021). Sex differences in the
670 association between major cardiovascular risk factors in midlife and dementia: A

671 cohort study using data from the UK Biobank. *BMC Medicine*, 19(1), 110.
672 <https://doi.org/10.1186/s12916-021-01980-z>

673 Goyal, K., Dumancic, S., & Blockeel, H. (2020). *Feature Interactions in XGBoost*
674 (arXiv:2007.05758). arXiv. <https://doi.org/10.48550/arXiv.2007.05758>

675 Grady, C. (2012). The cognitive neuroscience of ageing. *Nature Reviews Neuroscience*,
676 13(7), 491–505. <https://doi.org/10.1038/nrn3256>

677 Haufe, S., Meinecke, F., Görgen, K., Dähne, S., Haynes, J.-D., Blankertz, B., & Bießmann, F.
678 (2014). On the interpretation of weight vectors of linear models in multivariate
679 neuroimaging. *NeuroImage*, 87, 96–110.
680 <https://doi.org/10.1016/j.neuroimage.2013.10.067>

681 Jensen, J. H., Helpert, J. A., Ramani, A., Lu, H., & Kaczynski, K. (2005). Diffusional
682 kurtosis imaging: The quantification of non-gaussian water diffusion by means of
683 magnetic resonance imaging. *Magnetic Resonance in Medicine*, 53(6), 1432–1440.
684 <https://doi.org/10.1002/mrm.20508>

685 Kaden, E., Kelm, N. D., Carson, R. P., Does, M. D., & Alexander, D. C. (2016). Multi-
686 compartment microscopic diffusion imaging. *NeuroImage*, 139, 346–359.
687 <https://doi.org/10.1016/j.neuroimage.2016.06.002>

688 Karlsson, A., Rosander, J., Romu, T., Tallberg, J., Grönqvist, A., Borga, M., & Dahlqvist
689 Leinhard, O. (2015). Automatic and quantitative assessment of regional muscle
690 volume by multi-atlas segmentation using whole-body water-fat MRI. *Journal of*
691 *Magnetic Resonance Imaging: JMRI*, 41(6), 1558–1569.
692 <https://doi.org/10.1002/jmri.24726>

693 Kaufmann, T., van der Meer, D., Doan, N. T., Schwarz, E., Lund, M. J., Agartz, I., Alnæs,
694 D., Barch, D. M., Baur-Streubel, R., Bertolino, A., Bettella, F., Beyer, M. K., Bøen,
695 E., Borgwardt, S., Brandt, C. L., Buitelaar, J., Celius, E. G., Cervenka, S.,

696 Conzelmann, A., ... Westlye, L. T. (2019). Common brain disorders are associated
697 with heritable patterns of apparent aging of the brain. *Nature Neuroscience*, 22(10),
698 Article 10. <https://doi.org/10.1038/s41593-019-0471-7>

699 Kivimäki, M., Luukkonen, R., Batty, G. D., Ferrie, J. E., Pentti, J., Nyberg, S. T., Shipley, M.
700 J., Alfredsson, L., Fransson, E. I., Goldberg, M., Knutsson, A., Koskenvuo, M.,
701 Kuosma, E., Nordin, M., Suominen, S. B., Theorell, T., Vuoksimaa, E., Westerholm,
702 P., Westerlund, H., ... Jokela, M. (2018). Body mass index and risk of dementia:
703 Analysis of individual-level data from 1.3 million individuals. *Alzheimer's &*
704 *Dementia*, 14(5), 601–609. <https://doi.org/10.1016/j.jalz.2017.09.016>

705 Kolenic, M., Franke, K., Hlinka, J., Matejka, M., Capkova, J., Pausova, Z., Uher, R., Alda,
706 M., Spaniel, F., & Hajek, T. (2018). Obesity, dyslipidemia and brain age in first-
707 episode psychosis. *Journal of Psychiatric Research*, 99, 151–158.
708 <https://doi.org/10.1016/j.jpsychires.2018.02.012>

709 Kuo, C.-Y., Tai, T.-M., Lee, P.-L., Tseng, C.-W., Chen, C.-Y., Chen, L.-K., Lee, C.-K.,
710 Chou, K.-H., See, S., & Lin, C.-P. (2021). Improving Individual Brain Age Prediction
711 Using an Ensemble Deep Learning Framework. *Frontiers in Psychiatry*, 12, 308.
712 <https://doi.org/10.3389/fpsy.2021.626677>

713 Leonardsen, E. H., Peng, H., Kaufmann, T., Agartz, I., Andreassen, O. A., Celiuș, E. G.,
714 Espeseth, T., Harbo, H. F., Høgestøl, E. A., Lange, A.-M. de, Marquand, A. F., Vidal-
715 Piñeiro, D., Roe, J. M., Selbæk, G., Sørensen, Ø., Smith, S. M., Westlye, L. T.,
716 Wolfers, T., & Wang, Y. (2022). Deep neural networks learn general and clinically
717 relevant representations of the ageing brain. *NeuroImage*, 256, 119210.
718 <https://doi.org/10.1016/j.neuroimage.2022.119210>

719 Linge, J., Borga, M., West, J., Tuthill, T., Miller, M. R., Dumitriu, A., Thomas, E. L., Romu,
720 T., Tunón, P., Bell, J. D., & Dahlqvist Leinhard, O. (2018). Body Composition

721 Profiling in the UK Biobank Imaging Study: Body Composition Profiling in UK
722 Biobank. *Obesity*, 26(11), 1785–1795. <https://doi.org/10.1002/oby.22210>

723 López-Otín, C., Blasco, M. A., Partridge, L., Serrano, M., & Kroemer, G. (2013). The
724 Hallmarks of Aging. *Cell*, 153(6), 1194–1217.
725 <https://doi.org/10.1016/j.cell.2013.05.039>

726 Lundberg, S., & Lee, S.-I. (2017). *A Unified Approach to Interpreting Model Predictions*
727 (arXiv:1705.07874). arXiv. <https://doi.org/10.48550/arXiv.1705.07874>

728 Massy-Westropp, N. M., Gill, T. K., Taylor, A. W., Bohannon, R. W., & Hill, C. L. (2011).
729 Hand Grip Strength: Age and gender stratified normative data in a population-based
730 study. *BMC Research Notes*, 4, 127. <https://doi.org/10.1186/1756-0500-4-127>

731 Masters, R. K., Powers, D. A., & Link, B. G. (2013). Obesity and US Mortality Risk Over the
732 Adult Life Course. *American Journal of Epidemiology*, 177(5), 431–442.
733 <https://doi.org/10.1093/aje/kws325>

734 Maximov, I. I., Alnæs, D., & Westlye, L. T. (2019). Towards an optimised processing
735 pipeline for diffusion magnetic resonance imaging data: Effects of artefact corrections
736 on diffusion metrics and their age associations in UK Biobank. *Human Brain*
737 *Mapping*, 40(14), 4146–4162. <https://doi.org/10.1002/hbm.24691>

738 Maximov, I. I., van der Meer, D., de Lange, A.-M. G., Kaufmann, T., Shadrin, A., Frei, O.,
739 Wolfers, T., & Westlye, L. T. (2021). Fast quality control method for derived
740 diffusion metrics (YTTRIUM) in big data analysis: U.K. Biobank 18,608 example.
741 *Human Brain Mapping*, 42(10), 3141–3155. <https://doi.org/10.1002/hbm.25424>

742 Maximov, I. I., van der Meer, D., de Lange, A.-M., Kaufmann, T., Shadrin, A., Frei, O.,
743 Wolfers, T., & Westlye, L. T. (2020). *Fast quality control method for derived*
744 *diffusion metrics (YTTRIUM) in big data analysis: UK Biobank 18608 example*
745 [Preprint]. Neuroscience. <https://doi.org/10.1101/2020.02.17.952697>

746 Mielke, M. M., Bandaru, V. V. R., Haughey, N. J., Rabins, P. V., Lyketsos, C. G., & Carlson,
747 M. C. (2010). Serum sphingomyelins and ceramides are early predictors of memory
748 impairment. *Neurobiology of Aging*, *31*(1), 17–24.
749 <https://doi.org/10.1016/j.neurobiolaging.2008.03.011>

750 Miller, K. L., Alfaro-Almagro, F., Bangerter, N. K., Thomas, D. L., Yacoub, E., Xu, J.,
751 Bartsch, A. J., Jbabdi, S., Sotiropoulos, S. N., Andersson, J. L. R., Griffanti, L.,
752 Douaud, G., Okell, T. W., Weale, P., Dragonu, I., Garratt, S., Hudson, S., Collins, R.,
753 Jenkinson, M., ... Smith, S. M. (2016). Multimodal population brain imaging in the
754 UK Biobank prospective epidemiological study. *Nature Neuroscience*, *19*(11), 1523–
755 1536. <https://doi.org/10.1038/nn.4393>

756 Mori, S., Wakana, Nagae-Poetscher, & van Zijl, P. C. M. (2006). MRI Atlas of Human White
757 Matter. *AJNR: American Journal of Neuroradiology*, *27*(6), 1384–1385.

758 Nyberg, L. (2017). Neuroimaging in aging: Brain maintenance. *F1000Research*, *6*, 1215.
759 <https://doi.org/10.12688/f1000research.11419.1>

760 Pedregosa, F., Varoquaux, G., Gramfort, A., Michel, V., Thirion, B., Grisel, O., Blondel, M.,
761 Prettenhofer, P., Weiss, R., Dubourg, V., Vanderplas, J., Passos, A., Cournapeau, D.,
762 Brucher, M., Perrot, M., & Duchesnay, É. (2011). Scikit-learn: Machine Learning in
763 Python. *The Journal of Machine Learning Research*, *12*(null), 2825–2830.

764 Rodgers, J. L., Jones, J., Bolleddu, S. I., Vanthenapalli, S., Rodgers, L. E., Shah, K., Karia,
765 K., & Panguluri, S. K. (2019). Cardiovascular Risks Associated with Gender and
766 Aging. *Journal of Cardiovascular Development and Disease*, *6*(2), Article 2.
767 <https://doi.org/10.3390/jcdd6020019>

768 Ronan, L., Alexander-Bloch, A. F., Wagstyl, K., Farooqi, S., Brayne, C., Tyler, L. K., &
769 Fletcher, P. C. (2016). Obesity associated with increased brain age from midlife.

770 *Neurobiology of Aging*, 47, 63–70.
771 <https://doi.org/10.1016/j.neurobiolaging.2016.07.010>

772 Sanders, A.-M., Richard, G., Kolskår, K., Ulrichsen, K. M., Kaufmann, T., Alnæs, D., Beck,
773 D., Dørum, E. S., de Lange, A.-M. G., Egil Nordvik, J., & Westlye, L. T. (2021).
774 Linking objective measures of physical activity and capability with brain structure in
775 healthy community dwelling older adults. *NeuroImage: Clinical*, 31, 102767.
776 <https://doi.org/10.1016/j.nicl.2021.102767>

777 Schindler, L. S., Subramaniapillai, S., Barth, C., van der Meer, D., Pedersen, M. L.,
778 Kaufmann, T., Maximov, I. I., Linge, J., Leinhard, O. D., Beck, D., Gurholt, T. P.,
779 Voldsbekk, I., Suri, S., Ebmeier, K. P., Draganski, B., Andreassen, O. A., Westlye, L.
780 T., & de Lange, A.-M. G. (2022). Associations between abdominal adipose tissue,
781 reproductive span, and brain characteristics in post-menopausal women. *NeuroImage:*
782 *Clinical*, 36, 103239. <https://doi.org/10.1016/j.nicl.2022.103239>

783 Sebastiani, P., Thyagarajan, B., Sun, F., Schupf, N., Newman, A. B., Montano, M., & Perls,
784 T. T. (2017). Biomarker signatures of aging. *Aging Cell*, 16(2), 329–338.
785 <https://doi.org/10.1111/accel.12557>

786 Smith, S. M., Jenkinson, M., Johansen-Berg, H., Rueckert, D., Nichols, T. E., Mackay, C. E.,
787 Watkins, K. E., Ciccarelli, O., Cader, M. Z., Matthews, P. M., & Behrens, T. E. J.
788 (2006). Tract-based spatial statistics: Voxelwise analysis of multi-subject diffusion
789 data. *NeuroImage*, 31(4), 1487–1505.
790 <https://doi.org/10.1016/j.neuroimage.2006.02.024>

791 Stern, Y. (2009). Cognitive reserve. *Neuropsychologia*, 47(10), 2015–2028.
792 <https://doi.org/10.1016/j.neuropsychologia.2009.03.004>

793 Stern, Y. (2012). Cognitive reserve in ageing and Alzheimer’s disease. *The Lancet*
794 *Neurology*, 11(11), 1006–1012. [https://doi.org/10.1016/S1474-4422\(12\)70191-6](https://doi.org/10.1016/S1474-4422(12)70191-6)

795 Subramaniapillai, S., Suri, S., Barth, C., Maximov, I. I., Voldsbekk, I., van der Meer, D.,
796 Gurholt, T. P., Beck, D., Draganski, B., Andreassen, O. A., Ebmeier, K. P., Westlye,
797 L. T., & de Lange, A.-M. G. (2022). Sex- and age-specific associations between
798 cardiometabolic risk and white matter brain age in the UK Biobank cohort. *Human*
799 *Brain Mapping*, *n/a(n/a)*. <https://doi.org/10.1002/hbm.25882>

800 Tian, Y. E., Cropley, V., Maier, A. B., Lautenschlager, N. T., Breakspear, M., & Zalesky, A.
801 (2023). Heterogeneous aging across multiple organ systems and prediction of chronic
802 disease and mortality. *Nature Medicine*, 1–11. [https://doi.org/10.1038/s41591-023-](https://doi.org/10.1038/s41591-023-02296-6)
803 [02296-6](https://doi.org/10.1038/s41591-023-02296-6)

804 Tutor, A. W., Lavie, C. J., Kachur, S., Milani, R. V., & Ventura, H. O. (2023). Updates on
805 obesity and the obesity paradox in cardiovascular diseases. *Progress in*
806 *Cardiovascular Diseases*, *78*, 2–10. <https://doi.org/10.1016/j.pcad.2022.11.013>

807 Tyrrell, J., Zheng, J., Beaumont, R., Hinton, K., Richardson, T. G., Wood, A. R., Davey
808 Smith, G., Frayling, T. M., & Tilling, K. (2021). Genetic predictors of participation in
809 optional components of UK Biobank. *Nature Communications*, *12*(1), Article 1.
810 <https://doi.org/10.1038/s41467-021-21073-y>

811 Voldsbekk, I., Barth, C., Maximov, I. I., Kaufmann, T., Beck, D., Richard, G., Moberget, T.,
812 Westlye, L. T., & de Lange, A.-M. G. (2021). A history of previous childbirths is
813 linked to women’s white matter brain age in midlife and older age. *Human Brain*
814 *Mapping*, *42*(13), 4372–4386. <https://doi.org/10.1002/hbm.25553>

815 Wagenmakers, E.-J., Lodewyckx, T., Kuriyal, H., & Grasman, R. (2010). Bayesian
816 hypothesis testing for psychologists: A tutorial on the Savage–Dickey method.
817 *Cognitive Psychology*, *60*(3), 158–189.
818 <https://doi.org/10.1016/j.cogpsych.2009.12.001>

819 West, J., Romu, T., Thorell, S., Lindblom, H., Berin, E., Holm, A.-C. S., Åstrand, L. L.,
820 Karlsson, A., Borga, M., Hammar, M., & Leinhard, O. D. (2018). Precision of MRI-
821 based body composition measurements of postmenopausal women. *PloS One*, *13*(2),
822 e0192495. <https://doi.org/10.1371/journal.pone.0192495>

823 Wong, M. W., Braidy, N., Poljak, A., Pickford, R., Thambisetty, M., & Sachdev, P. S.
824 (2017). Dysregulation of lipids in Alzheimer's disease and their role as potential
825 biomarkers. *Alzheimer's & Dementia*, *13*(7), 810–827.
826 <https://doi.org/10.1016/j.jalz.2017.01.008>

827